TIME-RESOLVED ASSESSMENT OF EJECTA-MASS DISTRIBUTION USING 3D-PIV. B. Hermalyn[1], P. H. Schultz[1], J.L.B. Anderson[2] and J.T. Heineck[3], [1]Brown University, Providence, RI 02912-1846 (Brendan_Hermalyn@Brown.edu); [2]Winona State University, Winona, MN 55987; [3]NASA Ames Research Center, Moffet Field, CA 94035

Introduction: The ejecta mass from impact events affects the distribution and provenance of materials on planetary surfaces. Previous studies constrained the ejected mass through dimensional analysis [1], physical dissection [2,3,4], and experimental capture [5]. In this abstract, we discuss the development, utilization, and preliminary results of a novel noninvasive imaging technique for obtaining the time-resolved ejecta-mass distribution while in ballistic flight. Results are compared to prior studies [1,6].

Data Collection and Method: Impact experiments were conducted at the NASA Ames Vertical Gun Range (AVGR). As part of a general effort to understand ejecta-velocity distribution using Three-Dimensional Particle Imaging Velocimetry (3D-PIV), a new high-speed system imaged the advancing ejecta curtain at 1000fps (frames/sec). For initial calibration and proof of concept of the technique, 6.35 millimeter Aluminum projectiles were impacted into #20-40 sand at an angle of 90° (vertical) at both low (1 km/s) and high (5.4 km/s) velocities. In the application here, a horizontal (i.e. parallel to the target) pulsed laser light sheet was positioned at ~9 centimeters above the impact surface. The light sheet sliced the evolving cone-shaped ejecta curtain into a series of cross sections; two high speed, high-resolution CCD cameras captured these slices (Fig. 1). Since these images record the distribution of the particles in the curtain, the volume and mass of the ejecta can be determined at each time step. The 3D-PIV system uses a computer algorithm to cross-correlate individual particle motion, yielding the distance and direction, and thus velocity, of the ballistic ejecta.

Analysis and Results: The raw images collected were normalized and processed (through a routine of contrast stretching, brightness enhancement, and histogram matching) to yield binary 8-bit images that represent the cross sectional area of the ejecta curtain particles in the image. This strategy allowed particle and area counts of each image that were found to correlate with manual counts with accuracy of <10%. A representative area was chosen for particle and area counts to avoid undercounting due to shadow zones created by the optically thick ejecta curtain; this movable region of interest also allows future application to asymmetric oblique impacts.

Curtain width and radius. The ejecta curtain radius (Fig. 2) is measured from the impact point, which, in plan view for vertical impacts, is also the center of the flow field. By the nature of the measurements, the images are recorded at time $t=T_l+T_b$, where T_l is the time between impact and launch of ejecta and T_b is the ballistic time it takes the ejecta to ascend to the height of the laser sheet. The curtain radius is related to the horizontal velocity component of the ejected mass, the ejection angle of the curtain, and ejection position. The initial phase (before $t/T_c \sim 0.13$) in the 1 km/s impact is expressed by a large curtain radius (low ejection angle), not visible in the 5.4 km/s impact. The high speed material from the 5.4 km/s impact also arrives at the laser sheet height considerably sooner. The early-stage width (thickness) of the curtain (Fig. 3) is a difficult attribute to quantize due to sparse and finely comminuted ejecta. Both impacts exhibit a period of rapidly increasing width.

Volume and mass of ejecta: The number density (number of average sized particles in a specific region) is derived by dividing the total measured area of the particles and clumps illuminated (as in Fig. 1) in a defined region of interest by the average area of individual particles. Since the size and density of the target material is known, the volume and mass in each successive time step can be calculated from the number density.

To compare to prior studies, a cumulative volume of ejecta with higher velocity is calculated by fitting a curve to the discrete volumes at each time step and integrating. The 3D-PIV system allows the velocity for each time step to be calculated and plotted with the volume, permitting comparison to dimensional analysis and previous experiments (Fig. 4).

Conclusions: Initial results compare well to prior experiments [2,3] and accepted scaling laws [1], validating the proof of concept. The technique appears to reveal the transition from the early-stage coupling to later stage gravity-controlled excavation (Fig. 2).

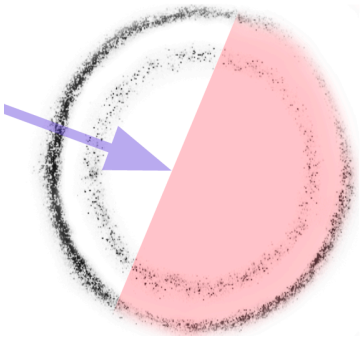

Figure 1. Ejecta curtain cross sections (inverted image). The rings correspond to different time steps of the same event in time steps 60ms apart (inner ring corresponds to earlier time) to show the growth and development of the ejecta curtain. Laser sheet illumination direction indicated by arrow. Note shadow zone denoted by red shading.

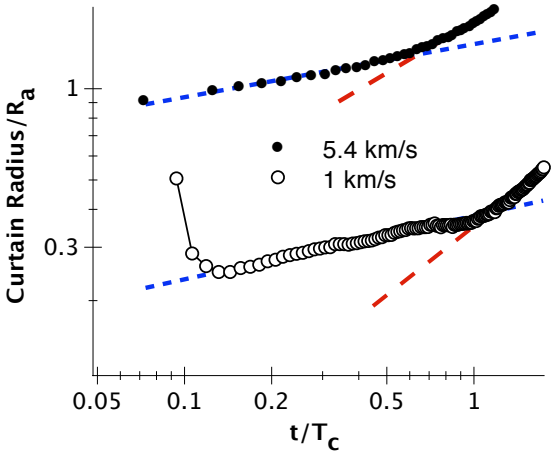

Figure 2. Ejecta curtain radius (measured from point of impact; nondimensional) vs. scaled time for 1km/s and 5.4km/s impact velocities into sand. Distinct phases in the growth of the curtain are shown with blue and red trendlines. Shift of hinge point (from t/T_c=1) is due to the ballistic time for the particles to reach the height of the laser sheet.

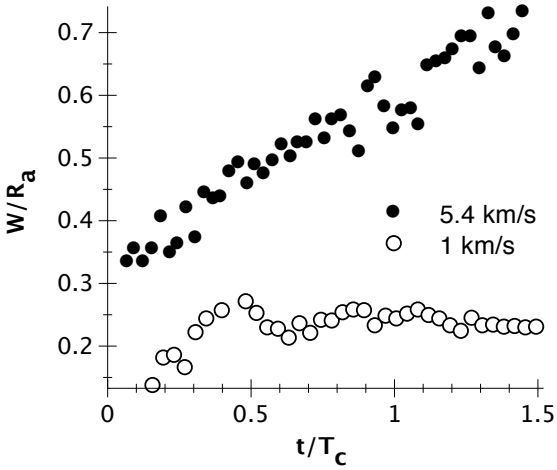

Figure 3. Ejecta curtain width (thickness) vs. t/T_c for same 1 km/s and 5.4 km/s impacts. The high-speed impact couples its energy and momentum fully and completely, whereas the lower speed impact exhibits a transition from initial coupling (penetration) to gravity-controlled excavation.

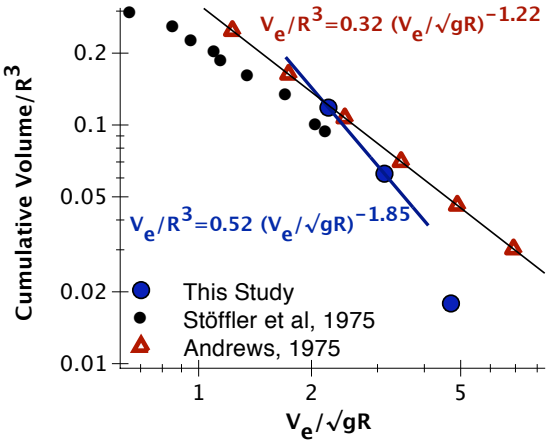

Figure 4. Cumulative nondimensional volume of ejecta with higher velocity. Blue points correspond to calculated volume; trendline in blue. Due to the thickness of the laser sheet, low-velocity materials may be over counted. This will be optimized in future experiments. For comparison, trends from explosion data in sand (red, from [Andrews, 1975]) and data for hypervelocity impacts into sand (from [Stöffler et al, 1975]) are shown.

References: [1] Housen, K.R., et al. (1983) *JGR, 88,* 2485-2499; [2] Andrews, R. J. (1975) *AFWL-TR-74-314*, 207; [3] Stöffler, D. et al. (1975) *JGR, 80,*4062-4077; [4] Morrison, R. H. and Oberbeck, V. R. (1976) *LPI Contributions, 259,* 79; [5] Schultz, P.H. (1996) *LPS XXX,* Abstract #1919; [6] Anderson, J.L.B., et al. (2003) *JGR, 108(E8),* 5094.